Supporting Information

Bioactive Profiling of Cowpea Pods via Optimized Extraction and Experimental–Computational Approaches

Maria Victoria Traffano-Schiffo[1], Margarita M. Vallejos [1,2],* Andrea G. Gómez[1], Beatriz I. Avalos[1], Belén A. Acevedo[1,2], María Victoria Avanza[1,2]

1 Instituto de Química Básica y Aplicada del Nordeste Argentino (IQUIBA-NEA), Consejo Nacional de Investigaciones Científicas y Técnicas (CONICET)-Universidad Nacional del Nordeste (UNNE), Avenida Libertad 5460, 3400, Corrientes, Argentina.
2 Facultad de Ciencias Exactas y Naturales y Agrimensura, Universidad Nacional del Nordeste (FaCENA-UNNE), Avenida Libertad 5460, 3400, Corrientes, Argentina

* Correspondence: m.vallejos@conicet.gov.ar; vallejos.marga@gmail.com

List of contents

-Table S1. Coded and real values and response variables for extraction optimization of phenolic compounds and antioxidant capacity of cowpea pods assisted by HIU and using ethanol solvent ……..…….....Page S2
-Table S2. Regression equations of the evaluated response variables total phenolic content and antioxidant capacity by $ABTS^{\bullet+}$…… Page S3
-Figure S1. Desirability, total phenolic content, and antioxidant capacity contour plots as a function of ethanol concentration (%), time (min) and high-intensity ultrasound amplitude (%) ……..……..... Page S3
-Figure S2. The fraction profile of (a) ethanolic and (b) aqueous extracts by Sephadex LH-20 column chromatography. Tubes 1-25 were eluted with 100 % ethanol and tubes 26-50 were eluted with 50 % ethanol-water solution ……... Page S4
-**Table S3.** Pearson's correlation test (r-values) between total phenolic content (TPC), and antioxidant capacity ……... Page S5
Theoretical Background and computational details
-Thermodynamic parameters related to antioxidative mechanisms……Page S6
-An overview of the quantum theory of atoms in molecules……Page S6
-Table S4. Bond dissociation enthalpies (BDE) for hydrogen atom of phenolic molecules in in kcal/mol……Page S7
-Figure S3. Molecular graph of the radicals stems of CA, CGA and QE, overlaid with their respective spin density distribution. ……..……. Page S8
-Table S5. Ionization potential (IP) and proton dissociation enthalpy (PDE). PDE values are provided for each site. Values are given in kcal/mol……..…….. Page S9
-Table S6. Proton affinity (PA) and electron transfer enthalpy (ETE) provided for each site. …….…… Page S9
References . ……..Page S10

Table S1. Real and coded values and response variables for extraction optimization of phenolic compounds and antioxidant capacity of cowpea pods assisted by HIU and using ethanol solvent.

Std	Run	Real and coded variables			Response variables	
		Ethanol concentration (%) (X_1)	HIU amplitude (%) (X_2)	time (min) (X_3)	Total Phenolic Content (mg_{GAE}/g) (Y_1)	Antioxidant Capacity-ABTS^{*+} ($mmol_{TE}/g$) (Y_2)
7	1	0 (-1)	40 (0)	20 (1)	30.9721	0.5322
13	2	25 (0)	40 (0)	12.5 (0)	33.6595	1.005
3	3	0 (-1)	80 (1)	12.5 (0)	40.4488	0.8976
6	4	50 (1)	40 (0)	5 (-1)	52.5796	1.123
10	5	25 (0)	80 (1)	5 (-1)	45.694	1.0098
12	6	25 (0)	80 (1)	20 (1)	32.7076	0.8574
9	7	25 (0)	0 (-1)	5 (-1)	30.7695	1.0835
15	8	25 (0)	40 (0)	12.5 (0)	35.5598	0.9742
2	9	50 (1)	0 (-1)	12.5 (0)	56.7255	1.2874
14	10	25 (0)	40 (0)	12.5 (0)	37.2049	1.1947
1	11	0 (-1)	0 (-1)	12.5 (0)	32.6717	0.5491
4	12	50 (1)	80 (1)	12.5 (0)	48.5971	1.1365
11	13	25 (0)	0 (-1)	20 (1)	48.6155	1.124
5	14	0 (-1)	40 (0)	5 (-1)	38.2046	0.9715
8	15	50 (1)	40 (0)	20 (1)	55.7292	1.2789

Table S2. Regression equations of the evaluated response variables total phenolic content and antioxidant capacity by $ABTS^{\bullet+}$.

	Intercept	X_1	X_2	X_3	X_1X_2	X_2X_3	X_{12}
Y1 = Total Phenolic Content (TPC, mgGAE/g)	37.74	8.92	-0.1668	0.0971	-3.98	-7.71	6.75
Y2 = Antioxidant Capacity $ABTS^{\bullet+}$ (AOC, mmolTE/g)	1.00	0.2344	-0.0178	-0.0494	-0.1248	0.1488	-

X_1 = Ethanol concentration (%); X_2 = HIU amplitude (%); X_3 = HIU treatment time (min).

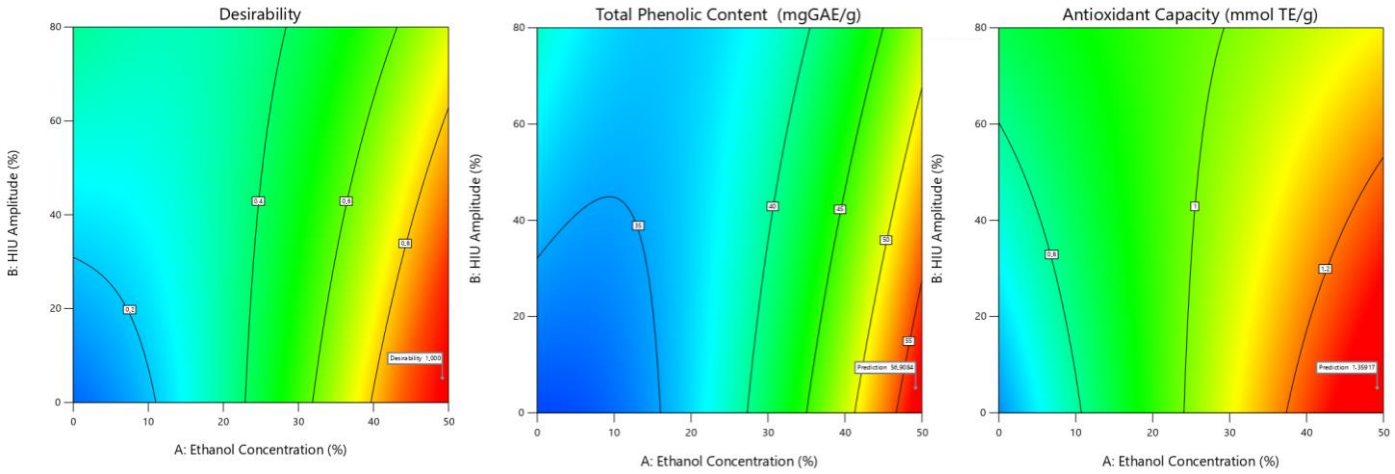

Figure S1. Desirability, total phenolic content, and antioxidant capacity contour plots as a function of ethanol concentration (%), time (min) and high-intensity ultrasound amplitude (%).

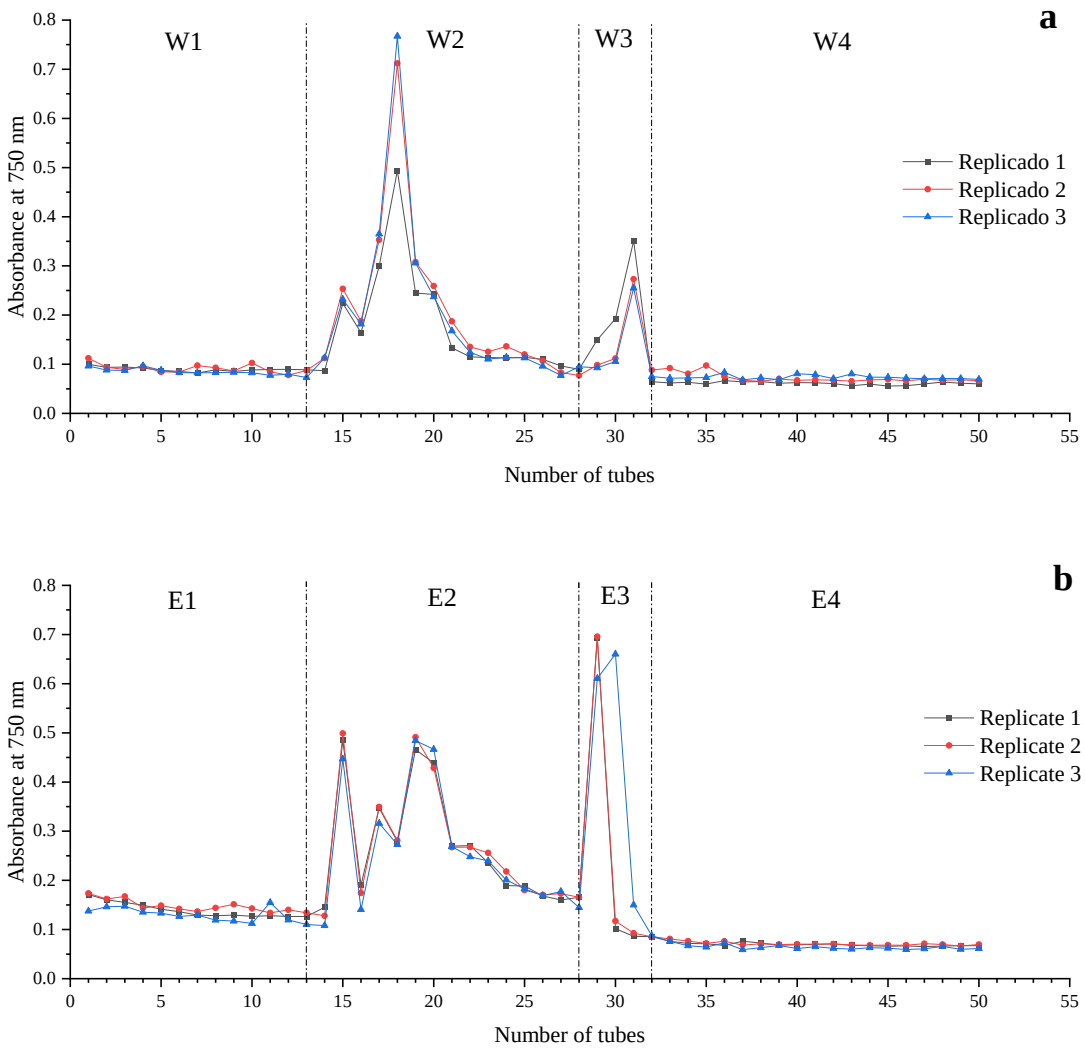

Figure S2. The fraction profile of (a) aqueous and (b) ethanolic extracts by Sephadex LH-20 column chromatography. Tubes 1-25 were eluted with 100 % ethanol and tubes 26-50 were eluted with 50 % ethanol-water solution.

Table S3. Pearson's correlation test (*r*-values) between total phenolic content (TPC), and antioxidant activities (obtained from DPPH and FRAP assays) for ethanolic (E) and aqueous (W) extract and fractions.

Samples	DPPH	FRAP
E	0.9774*	0.9774*
W	0.9360*	0.5924

*Correlation is significant at $p < 0.05$

The results from Tabla S3 revealed a significant correlation ($p < 0.05$) between TPC and AOC (measured by both DPPH and FRAP) for the ethanolic extract (E0) and its fractions (E1–E4). However, for the aqueous extract (W0) and its fractions (W1–W4), a significant correlation ($p < 0.05$) was observed only between TPC and DPPH values. The correlation between TPC and FRAP was moderate ($r = 0.5924$) and not statistically significant ($p > 0.05$). In agreement with the literature, these results suggest that phenolic compounds present in the extracts and fractions contribute significantly to their AOC, although other compounds and factors may also play a role [1].

Theoretical Background and Computational Details

-Thermodynamic parameters related to antioxidative mechanisms

Density functional theory (DFT) study was performed in order to provide a better understanding of the relationship between the compounds detected in the extracts and the antioxidant activity.
The main mechanisms proposed to explain the radical scavenging ability of phenolic antioxidants are [2]:

1. Hydrogen atom transfer (HAT) from antioxidant molecules (ArOH) to radicals ($R^{\bullet}$), Eq 1

$$ArOH + R\bullet \rightarrow ArO\bullet + RH \quad (1)$$

2. Two-step reaction: single-electron transfer followed by proton transfer (SET-PT), Eq 2

$$ArOH + R\bullet \rightarrow ArOH{+}\bullet + R{-} \rightarrow RH + ArO\bullet \quad (2)$$

3. Two-step reaction: sequential proton loss electron transfers (SPLET), Eq 3

$$ArOH \rightarrow ArO^{-} + H^{+};\ ArO^{-} + R^{\bullet} \rightarrow ArO^{\bullet} + R^{-};\ R^{-} + H^{+} \rightarrow RH \quad (3)$$

Theoretical methods can be employed to estimate various numerical parameters associated with three mechanisms, namely bond dissociation enthalpy (BDE), ionization potential (IP), proton dissociation enthalpy (PDE), proton affinity (PA), and electron transfer enthalpy (ETE). The following equations describe these parameters:

$$BDE = H(ArO^{\bullet}) + H(H^{\bullet}) - H(ArOH) \quad (4)$$

$$IP = H(ArOH^{\bullet+}) + H(e^{-}) - H(ArOH) \quad (5)$$

$$PDE = H(ArO^{\bullet}) + H(H^{+}) - H(ArOH^{\bullet+}) \quad (6)$$

$$PA = H(ArO^{-}) + H(H^{+}) - H(ArOH) \quad (7)$$

$$ETE = H(ArO^{\bullet}) + H(e^{-}) - H(ArO^{-}) \quad (8)$$

where *H* is molecular enthalpy of different species. In the HAT pathway, the reactivity of ArOH can be determined by using BDE parameter (eq 4). For SET-PT mechanism, IP and PDE of $ArOH^{\bullet+}$are the defining parameters. In the SPLET mechanism, the radical scavenging activity, can be explaining by considering the first step reaction enthalpy, PA and ETE.
For the calculation the *H* ($H^{\bullet}$), *H* (H^{+}) and *H* (e^{-}) in methanol were obtained from the literature [3].

An overview of the quantum theory of atoms in molecules

The quantum theory of atoms in molecules (QTAIM) is based on the topological analysis of the electron charge density, which allows for the prediction of molecular structure and facilitates comparison of across a range molecular system [4, 5]. The analysis focuses on the on the critical points of the electronic density distribution within topological QTAIM approach. At a bond critical point (bcp), the properties of the charge density provide valuable insights into the nature and characteristics of a bonding interaction. The strength of a bond can be estimated from the electron charge density (ρ_b) at the bcp, while its Laplacian function ($\nabla^2\rho_b$) provides information on local charge concentration (($\nabla^2\rho_b < 0$) or local charge depletion (($\nabla^2\rho_b > 0$). In hydrogen bonding interactions, the values of ρ_b range from 0.002 to 0.040 au, while the values of $\nabla^2\rho_b$ range from 0.020 to 0.150 au.[6].

Spin density is a measure of the distribution of unpaired electrons in a molecule or radical species.
The spin density distribution is a reasonably reliable parameter for providing a better representation of the stability evaluating the stability of radical species. In general, radical species with more spin density are more stable because the unpaired electrons are more delocalized and less reactive. This is because the electrons are spread out over a larger area, which makes it more difficult for them to interact with other molecules or radicals.
On the other hand, the distribution of the Laplacian of the electron density ($(\nabla^2\varrho)$ is a powerful tool in the interpretation of quantum chemical results. It provides an enhanced view of the regions wherein the charge density is concentrated or depleted in a molecular system [4]. The topological QTAIM analysis, including the population of atomic spin densities [3], was carried out using the AIMALL program [7] as a useful tool to analyze and compare electron density distributions of molecular systems.

HAT mechanism

Table S4. Bond dissociation enthalpies (BDE) for hydrogen atom of phenolic molecules in kcal/mol.

PC	Position	Gas	Methanol	Ethanol	Water
p-Coumaric acid (pCoA)	4-OH	81.2	82.4	83.0	83.3
Caffeic acid (CA)	3-OH	84.7	81.5	81.5	82.2
	4-OH	73.0	76.5	76.5	77.4
Caftaric acid (CtA)	3-OH	83.9	80.5	81.1	81.2
	4-OH	72.6	76.0	76.4	76.9
Morin (Mo)	3-OH	75.5	73.7	73.7	74.5
	5-OH	95.1	88.2	88.8	89.1
	7-OH	87.4	87.2	87.3	88.0
	2′-OH	87.6	84.4	84.5	85.4
	4′-OH	84.2	83.9	83.9	84.6

Table S3 shows the calculated BDEs for the phenolic compounds in the gas phase, ethanol, and water. The BDEs range from 72.6 to 95.1 kcal/mol, in agreement with previous theoretical studies on similar systems [8].
The OH group at the *para* position (4-OH) shows the lowest BDE values for CA and CtA compounds, suggesting it is the most reactive site in all the solvents studied, following HAT pathway. For morin, there are five possible sites. The BDE values increase in the order: 3-OH < 4′-OH < 7-OH < 2′-OH < 5-OH, indicating that the 3-OH group on the C-ring is the most reactive site.
The ability of these compounds to undergo hydrogen abstraction is only slightly affected by polar solvents. Although the BDE values clearly highlight the most reactive sites and compounds in both gas and solution phases, they do not provide a direct explanation for these observations
The stability of the radicals generated by homolytic cleavage of the O-H bond can be better understood by examining the spin density distribution on the phenoxyl oxygen. A lower spin density suggests greater delocalization of the unpaired electron, leading to enhanced radical stability. Figure S3 presents the spin density distributions for the potential radical species formed from homolytic O-H bond cleavage in CA, CtA, and Mo.

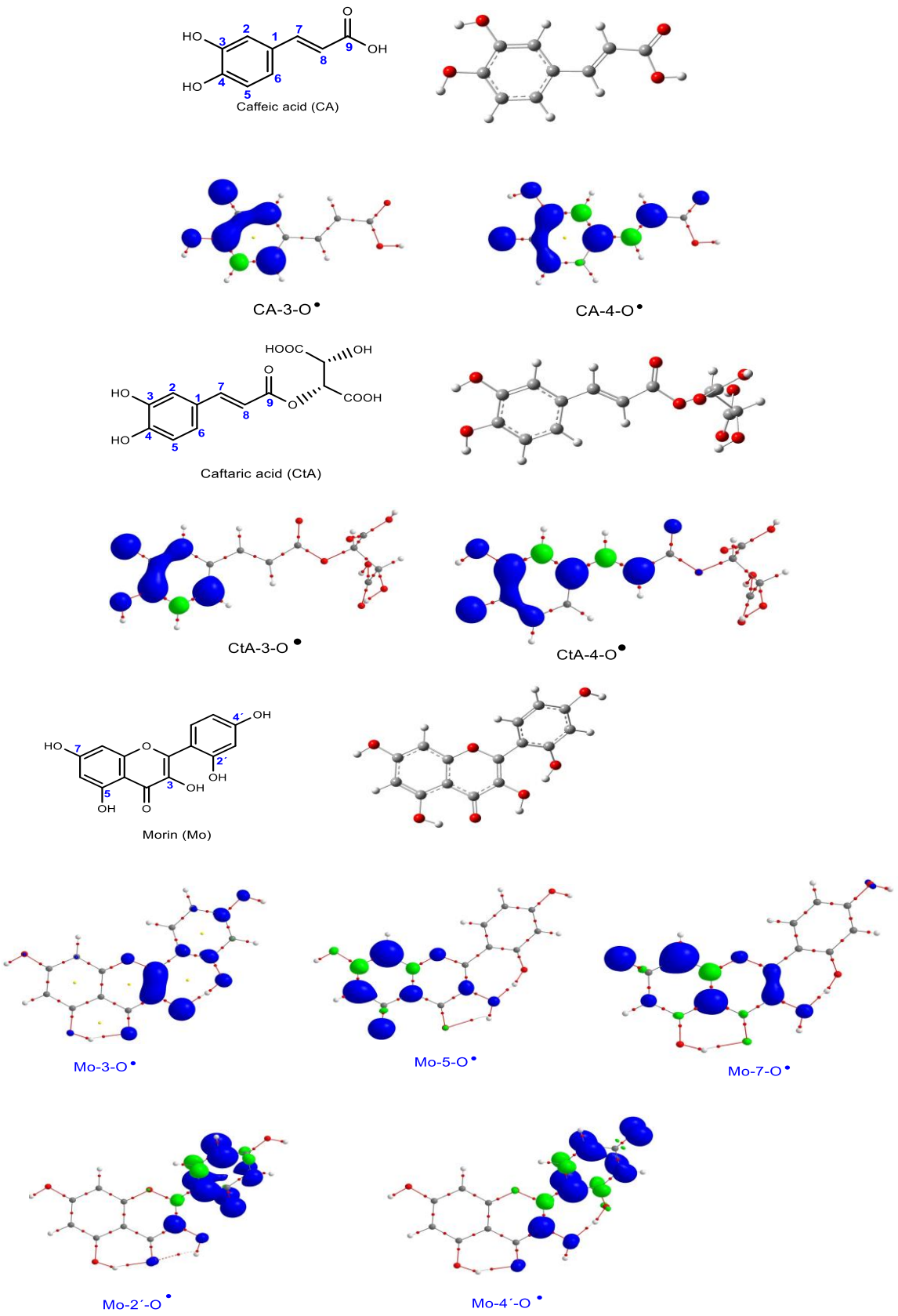

Figure S3. Molecular graph of the radicals stems of CA, CGA and QE, overlaid with their respective spin density distribution.

SET-PT mechanism

Table S5. Ionization potential (IP) and proton dissociation enthalpy (PDE). PDE values are provided for each site. Values are given in kcal/mol

	IP					PDE			
PC	Gas	Metha-nol	Etha-nol	Water	position	Gas	Methanol	Ethanol	Water
pCoA	185.1	116.4	117.4	111.0	4-OH	212.1	6.4	5.8	9.4
CA	182.7	112.8	114.0	108.1	3-OH	218.1	9.2	7.8	11.3
					4-OH	206.4	4.1	2.5	6.5
CtA	179.3	112.7	113.7	107.3	3-OH	220.5	8.3	7.7	11.1
					4-OH	209.2	3.8	3.1	6.8
Mo	171.3	111.2	111.6	106.1	3-OH	220.1	2.9	2.4	5.5
					5-OH	299.9	17.4	17.5	20.1
					7-OH	292.2	16.4	16.0	19.0
					2′-OH	292.4	13.6	13.2	16.4
					4′-OH	289.0	13.1	12.6	15.6

Table S4 reports the calculated IPs and PDEs of the four PCs in the gas phase, EtOH, MeOH and H_2O solutions.
The data reveal that the IP values range between 171.3 and 182.7 kcal/mol in the gas phase, and between 113.7 and 106.1 kcal/mol in solution. IPs are global parameters influenced by the structure of the entire molecule. The ranking of antioxidant capacity, when considering the solvent, shows some differences compared to the evaluation based on BDE, which is a local parameter dependent on the relative positions of substituents [9, 10]. Notably, the IP values decrease significantly in polar media compared to the gas phase, indicating that polar solvents greatly promote electron transfer to free radicals, thereby enhancing antioxidant activity.
The PDE defines the second step of the SET–PT mechanism and helps identify the thermodynamically favoured OH group for deprotonation from the cation radical. As shown in Table S4, the lowest PDE for CA and CtA corresponds to the 4-OH group in the para position, while for Mo, it is associated with the 3-OH group. These findings are consistent with the results obtained from BDEs. Like IP values, there is a significant reduction in PDEs in solution compared to the gas phase, which can be attributed to the strong stabilisation of the positively charged proton in polar solvents.

SPLET mechanism

Table S6. Proton affinity (PA) and electron transfer enthalpy (ETE) provided for each site.

		PA				ETE			
PC	posi-tion	Gas	Methanol	Etha-nol	Water	Gas	Methanol	Ethanol	Water
pCoA	4-OH	326.5	31.6	30.3	33.0	70.6	91.2	89.9	87.4
CA	3-OH	324.4	35.0	36.7	35.9	76.2	86.9	85.1	83.5
	4-OH	318.6	27.9	28.7	29.3	70.3	89.0	87.9	85.2
CtA	3-OH	338.3	35.0	37.6	36.1	61.5	85.7	83.8	82.2
	4-OH	317.2	28.0	29.6	29.5	71.3	88.4	87.2	84.5
Mo	3-OH	320.4	25.0	26.0	26.1	71.1	89.1	88.0	85.6
	5-OH	336.4	34.8	36.6	36.0	74.6	93.8	92.5	90.2
	7-OH	323.2	29.9	31.1	31.2	80.1	97.6	96.5	93.9
	2′-OH	334.7	33.6	35.4	34.9	68.8	91.1	89.4	87.6
	4′-OH	326.6	32.3	33.6	33.6	73.5	92.0	90.6	88.2

Values are given in kcal/mol.

In both the gas phase and solutions (methanol, ethanol, and water), the 4-OH group of CA and CtA, and the 3-OH group of Mo exhibit the lowest PA values, making them the most likely candidates for heterolytic cleavage. Since the radical anion and proton are much more stabilised in solution compared to the gas phase, the PA values in the gas phase are high, decreasing significantly when evaluated in polar solvents.

Following proton dissociation, the next step in the SPLET mechanism involves electron transfer from ArO– to the free radical. The ability to release this electron density, measured by ETE, indicates how readily the anionic form of the antioxidant can complete this step. In the gas phase, the 3-OH group of CA shows lower ETE values than the 4-OH group. Conversely, for CtA, the 4-OH group has the lowest ETE. For Mo, the 3-OH group consistently shows the lowest ETE across all environments studied.

References

1. Avalos, B.I., Ojeda, G.A., Spinnenhirn, E.D., Acevedo, B.A., and Vallejos, M.M. "Evaluation of Phenolic Compounds and Antioxidant Capacity in Mucuna Pruriens and Cajanus Cajan Pods Extracts." *Food Chem. Adv.* **2023**, 3, 100503.
2. Leopoldini, M., Russo, N., and Toscano, M. "The Molecular Basis of Working Mechanism of Natural Polyphenolic Antioxidants." *Food Chem.* **2011**, 125, 288-306.
3. Marković, S., and Tošović, J. "Comparative Study of the Antioxidative Activities of Caffeoylquinic and Caffeic Acids." *Food Chem.* **2016**, 210, 585-92.
4. Bader, R.F.W. *Atoms in Molecules. A Quantum Theory*. London Oxford Science Publications, Clarendon Press, **1990**.
5. Matta, C.F., Arabi, A.A., and Keith, T.A. "Atomic Partitioning of the Dissociation Energy of the P-O(H) Bond in Hydrogen Phosphate Anion (Hpo_4^{2-}): Disentangling the Effect of Mg^{2+}." *J. Phys. Chem. A* **2007**, 111, 8864-72.
6. Popelier, P.L.A. *Atoms in Molecules. An Introduction,* . Harlow, UK: Pearson Education, **2000**.
7. Aimall Version Version 11.12.19. TK Gristmill Software, Overland Park KS, USA.
8. Leopoldini, M., Rondinelli, F., Russo, N., and Toscano, M. "Pyranoanthocyanins: A Theoretical Investigation on Their Antioxidant Activity." *J. Agric. Food Chem.* **2010**, 58, 8862-71.
9. Wright, J.S., Johnson, E.R., and DiLabio, G.A. "Predicting the Activity of Phenolic Antioxidants: Theoretical Method, Analysis of Substituent Effects, and Application to Major Families of Antioxidants." *J. Am. Chem. Soc.* **2001**, 123, 1173-83.
10. Shang, Y., Li, X., Li, Z., Zhou, J., Qu, L., and Chen, K. "Theoretical Study on the Radical Scavenging Activity and Mechanism of Four Kinds of Gnetin Molecule." *Food Chem.* **2022**, 378, 131975.